

Parameters identification of HIV dynamic models for HAART treated patients: a comparative study

Marco Laurino, Alberto Landi and Gabriele Pannocchia

Abstract—We present a comparative study of parameters identification of HIV dynamic models for naive patients that are treated with two different HAART (Highly Active Anti-Retroviral Therapy) protocols during a period of 48 weeks. Three HIV models of increasing complexity (in terms of number of state variables and parameters) have been chosen, and for each one the model parameters are computed by solving a nonlinear optimization problem via sequential quadratic programming (SQP). Model parameters are divided into “group dependent”, common to all patients treated with same HAART protocol, and “patient dependent”, specific for each patient, and are estimated in a way that an overall cost function comprising the fitting error of CD4+ concentration and viral load measurements. A preliminary parameter space grid search algorithm is performed in order to find a suitable initial guess for the SQP algorithm. Numerical results indicate that all considered models can give a good matching despite the scarcity of available measurements for each patient, and in this limited situation the minimal model appears to be (slightly) more effective than the other models.

I. INTRODUCTION

In a historical paper [1] presenting mathematical models of HIV disease, Perelson and Nelson claimed that a number of stochastic and deterministic models have been developed to describe the immune system, its interaction with HIV, and the decline in CD4+ T cells. They added the comment: ‘These models typically consider the dynamics of the CD4+ T cell and virus populations as well as the effects of drug therapy. In some of these models other immune system populations, such as macrophages or CD8+ cells, have been included. Many of these models have tended to focus on explaining the kinetics of T cell decline. Unfortunately, many different models have been able to, more or less, mimic this aspect of HIV infection, and to make progress, additional criteria needed to be developed.’

From 1999 many other HIV dynamical models have been proposed in the literature mainly for two reasons. The first one is that they usually show a positive impact on the understanding of HIV infection and can predict in silico the effects of administration of drugs. The second one has a less worthwhile goal, due to the application of a merely mathematical exercise to a fashionable problem. The question introduced in [1] on the usefulness of the models is very complex to be answered: in this paper we attempt to investigate this topic.

M. Laurino is with Department of Surgery, Medical, Molecular, and Critical Area Pathology, Univ. of Pisa, Italy (marco.laurino@for.unipi.it). A. Landi is with Department of Information Engineering, Univ. of Pisa, Italy (landi@ieee.org). G. Pannocchia is with Department of Civil and Industrial Engineering, Univ. of Pisa, Italy (g.pannocchia@diccism.unipi.it). Corresponding author.

Nevertheless a similar problem is common to other aspects of HIV research, e.g. in epidemiology, where a systematic study of twelve mathematical models of the potential impact of antiretroviral therapy on HIV incidence have been recently published [2].

In this paper we propose a comparative study of parameters identification of HIV dynamic models, limiting our analysis to three models. The first model we considered is the earliest three-state variable model (see [3], [4] and references therein). Two variants are considered for comparison: they take the immune system response into account by adding variables associated with cytotoxic lymphocytes. The first variant represents a classical model in literature (e.g. [5], [6]), the other one includes the virulence based approach [7]–[9]).

II. HIV MODELS

In this work we consider and compare three HIV models of increasing complexity in terms of number of state variables (as well as of parameters). We present the details of each model next, and we highlight for each how the effect of HAART is taken into account. Each model can be written in the following general form:

$$\begin{aligned}\dot{\mathbf{x}} &= F(\mathbf{x}, f, \boldsymbol{\theta}) \\ \mathbf{y} &= H(\mathbf{x}, \boldsymbol{\theta}),\end{aligned}\tag{1}$$

in which $\mathbf{x} \in \mathbb{R}^{n_x}$ is the state variable vector, $\mathbf{y} \in \mathbb{R}^{n_y}$ is the measured output vector, $f \in \{0, 1\}$ is the normalized drug amount (where 0 means no therapy and 1 means HAART therapy), $\boldsymbol{\theta} \in \mathbb{R}^L$ is the vector of parameters. $F : \mathbb{R}^{n_x} \times \mathbb{R} \times \mathbb{R}^L \rightarrow \mathbb{R}^{n_x}$ and $H : \mathbb{R}^{n_x} \times \mathbb{R}^L \rightarrow \mathbb{R}^{n_y}$ are assumed to be continuous.

A. Model 1: minimal model

The simplest HIV model, proposed in [4], is described by the following set of ordinary differential equations:

$$\begin{cases} \dot{x} = \lambda - dx - \beta xv \\ \dot{y} = \beta xv - ay \\ \dot{v} = ky - uv. \end{cases}\tag{2}$$

In (2), x is the concentration of healthy CD4+ T cells, y is the concentration of infected CD4+ T cells, and v is the concentration of free virus, often referred to as the viral load. Healthy CD4+ (x) are produced with rate λ , naturally die with rate dx and become infected with rate βxv . That is the rate of infection is proportional to both healthy CD4+ and virus concentrations. Consequently, infected CD4+ (y) are produced with rate βxv and naturally die with rate

ay. Free virus (v) is produced with rate ky and naturally dies with rate uv . As discussed in [3], [10], model (2) is completely identifiable, which means that all parameters can be calculated from the measured output. This property clearly refers to the noise-free case, although convergence in the presence of noise may also be established [10].

The effect of HAART can be included in model (2) by reducing the infection rate constant as follows: $\beta \leftarrow \beta(1 - \eta f)$, in which $\eta \in (0, 1)$ is drug effectiveness. Hence the considered model is as follows:

$$\text{Model 1: } \begin{cases} \dot{x} = \lambda - dx - \beta(1 - \eta f)xv \\ \dot{y} = \beta(1 - \eta f)xv - ay \\ \dot{v} = ky - uv. \end{cases} \quad (3)$$

We notice that this model is in the form of (1) by defining: $\mathbf{x} = [x \ y \ v]'$, $\boldsymbol{\theta} = [\lambda \ d \ \beta \ \eta \ a \ k \ u]'$ and $\mathbf{y} = [x \ v]'$, since we assume that the measured variables are the concentration of healthy CD4+ cells and the viral load. Functions $F(\cdot)$ and $H(\cdot)$ are consequently defined.

B. Model 2: including immune system response variables

Research on HIV control has focused on identifying therapy protocols able to result in long-term immune-mediated control of HIV. In particular, cytotoxic T lymphocyte (CTL) responses have been shown to be particularly effective in reducing HIV replication rate. These immune responses have been captured by the following mathematical model [6]:

$$\begin{cases} \dot{x} = \lambda - dx - \beta xv \\ \dot{y} = \beta xv - ay - pyz \\ \dot{w} = cxyw - cqyw - bw \\ \dot{z} = cqyw - hz, \end{cases} \quad (4)$$

in which, in addition to healthy and infected CD4+ T cells (x and y , respectively), w represents the CTL precursors and z are the CTL effectors, which are ultimately responsible for killing infected cells with a rate pyz . Compared to model (2), the viral load is not explicitly described because it is generally assumed that $\dot{v} = ky - uv \sim 0$, and hence $v \sim \frac{k}{u}y = \bar{k}y$, i.e. the viral load is proportional to the infected CD4+ T cells. CTL precursors proliferate at rate $cxyw$, die at rate bw , and differentiate into CTL effectors at rate $cqyw$. CTL effectors die at rate hz . From a physiological point of view, one should expect model (4) to describe the HIV dynamics better than model (2) because the former takes into account the CTL immune responses which are known to play an important role in the success of HIV control [6], especially if a significant amount of CTL precursors is reached early. On the other hand, model (4) has four parameters more than (2) to identify.

As in model (2), the effect of HAART is modeled by replacing $\beta \leftarrow \beta(1 - \eta f)$ obtaining:

$$\text{Model 2: } \begin{cases} \dot{x} = \lambda - dx - \beta(1 - \eta f)xy \\ \dot{y} = \beta(1 - \eta f)xy - ay - pyz \\ \dot{w} = cxyw - cqyw - bw \\ \dot{z} = cqyw - hz. \end{cases} \quad (5)$$

The general form (1) is clearly obtained by defining: $\mathbf{x} = [x \ y \ w \ z]'$, $\mathbf{y} = [x \ v]'$, and $\boldsymbol{\theta} = [\lambda \ d \ \beta \ \eta \ a \ p \ c \ q \ b \ h \ \bar{k}]'$. Function $F(\cdot)$ is readily defined from (5) whereas $H(\cdot)$ is given by:

$$H(\mathbf{x}, \boldsymbol{\theta}) = \begin{bmatrix} x \\ \bar{k}y \end{bmatrix}. \quad (6)$$

C. Model 3: including immune system response variables and increasing virulence

One possible criticism regarding the two models previously presented is that they admit stable equilibrium points in absence of therapy, i.e. they admit the possibility to stop permanently anti-retroviral therapy without any eventual uptake of viral load and fall of healthy CD4+ T cells. As secondary aspect, neither model (3) nor (5) discriminate between the effects of Protease Inhibitors (PI) and Reverse Transcriptase Inhibitors (RTI) used (together) in HAART protocols. This observation led Landi et al. [9] to propose a variant of (4) in which infection rate constant β is replaced by an additional state which (slightly) grows linearly with time. Such a state, referred to as *virulence*, makes the system evolution uncontrollable after many years (decades). According pharmacological considerations, the effect of PI is modeled as a reduction of the free virus production rate from infected cells, whereas the effect of RTI is modeled as a reduction of virulence growth rate. Recently Pannocchia et al. [7] argued that an indefinite linear growth of the virulence state, even if extremely slow, may not be justified from a biological perspective. As a remedy the purely integrating dynamics of the virulence state was replaced by a stable linear dynamics in which the steady state virulence value is such that the system still does not admit stable equilibria.

The model considered in [7] is described by:

$$\begin{cases} \dot{x} = \lambda - dx - rxv \\ \dot{y} = rxv - ay - pyz \\ \dot{v} = k(1 - \eta_P f)y - uv \\ \dot{w} = cxyw - cqyw - bw \\ \dot{z} = cqyw - hz \\ \dot{r} = (1 - \eta_T f)(b_r - a_r r), \end{cases} \quad (7)$$

in which r is the virulence dynamic state, $\eta_P \in (0, 1)$ is PI drug effectiveness, $\eta_T \in (0, 1)$ is the RTI drug effectiveness. We can notice that the infection rate is now rxv , and r follows a first-order dynamics:

$$r(t) = r(t_0) \exp\left(-\frac{t-t_0}{\tau}\right) + \left(\frac{b_r}{a_r}\right) \left(1 - \exp\left(-\frac{t-t_0}{\tau}\right)\right), \quad (8)$$

in which $\tau = \frac{1}{(1-\eta_T f)a_r}$ is the first-order time constant. It is easy to notice that $\lim_{t \rightarrow \infty} r(t) = r_\infty = \frac{b_r}{a_r}$. Moreover, since $r(t_0)$ is chosen smaller than r_∞ , the virulence grows with time and asymptotically reaches a constant value. The effect of RTIs is modeled as reduction of the virulence growth rate by a factor $(1 - \eta_T f)$, i.e. an increase of first-order time

constant. We here propose a minor variant to model (7):

$$\text{Model 3: } \begin{cases} \dot{x} = \lambda - dx - (1 - \eta_T f)rxv \\ \dot{y} = (1 - \eta_T f)rxv - ay - pyz \\ \dot{v} = k(1 - \eta_P f)y - uv \\ \dot{w} = cxyw - cqyw - bw \\ \dot{z} = cqyw - hz \\ \dot{r} = b_r - a_r r. \end{cases} \quad (9)$$

We notice that according to (9), the virulence state r still evolves as in (8) with $\tau = \frac{1}{a_r}$, i.e. the first-order time constant is not affected by RTI drugs. On the other hand, the infection term is reduced by a factor $(1 - \eta_T f)$ due the effect of RTI drugs, similarly to models (3) and (5).

The general form (1) is obtained by defining: $\mathbf{x} = [x \ y \ v \ w \ z \ r]'$, $\mathbf{y} = [x \ v]'$, and $\boldsymbol{\theta} = [\lambda \ d \ \eta_P \ \eta_T \ a \ p \ c \ q \ b \ h \ k \ u \ a_r \ b_r]'$. Functions $F(\cdot)$ and $H(\cdot)$ are consequently defined from (9). Clearly, in comparison with models (3) and (5), model (9) is more involved in terms of number of states and parameters to be identified.

III. PARAMETERS IDENTIFICATION

In order to compare models of different complexity, for each model a similar identification procedure has been followed, which is based on the minimization of the weighted sum of square errors of fitting for CD4+ T cell concentration and viral load. The key aspects of the identification procedure, common to all models, are: (i) the model parameters are divided into group dependent parameters (i.e. identical for all patients under the same treatment) and patient dependent parameters (i.e. specific for each patient); (ii) the date of seroconversion is not known, and it is also estimated for each patient as additional parameter; (iii) an initial suboptimal combination of group and patients parameters is obtained by discretizing the parameters space and performing a grid search; (iv) starting from the suboptimal combination of parameters found in (iii), a constrained nonlinear optimization problem is solved using an SQP algorithm to achieve further reduction of the objective function.

A. Datasets

Data of patients used in this work were provided by the San Raffaele Research Institute (Milano, Italy) within the VEMAN Study [11]. More specifically, two groups of patients are considered:

- **TRU.** Patients treated with a standard HAART protocol composed by a PI and Truvada (typical RTI).
- **MVC.** Patients treated with an experimental HAART protocol composed by a PI and Maraviroc.

In both groups all patients are naive, i.e. never treated with HAART protocols before, and they are monitored for 48 weeks after the beginning of therapy measuring, among other plasma indicators not used in this work, concentration of CD4+ T cells and free virus at week 0, 4, 8, 16, 24, 36, and 48. The measurements at week 0 are collected just before the starting of the therapy.

The VEMAN study comprises 25 patients of each group, but in this work we considered 11 patients of the TRU group and 14 patients of the MVC group because for other patients the full period of 48 was not reached. It is also important to remark that in most cases after a few months of HAART the viral load falls below the detection limit of 36 copies/mL, values that is returned by the instrument for any actual concentration lower or equal to that limit.

B. Identification problem rationale and formulation

Given the different mechanism of action of the drugs used in the two groups, we perform separate parameter identification for each group. Adopting a similar rationale as in [7] for each model we grouped the parameters as follows:

- some parameters are regarded identical for all patients of the group, and define the vector $\boldsymbol{\theta}_g$;
- some parameters are regarded specific for each patient, and define the vector $\boldsymbol{\theta}_i$ for the i -th patient;
- some parameters are not identified and their value is taken from the literature; they define the vector $\boldsymbol{\theta}_0$.

Hence, for each model describing the HIV evolution in the i -th patient the overall parameters vector is given by:

$$\boldsymbol{\theta} = [\boldsymbol{\theta}'_0 \ \boldsymbol{\theta}'_g \ \boldsymbol{\theta}'_i]'. \quad (10)$$

The choice of considering some parameters identical for all patients in the same group, as well as assuming known from the literature some other parameters is motivated by:

- the partial identifiability of Model 2 and Model 3 opposed to global identifiability of Model 1 [7], [10];
- the limited number of available measurements (14 measurements for each patient);
- the impossibility of choosing the sampling instants;
- the limited information contained in many samples of viral load, which are below the detection limit.

Furthermore, the datasets include only one measurement prior to the beginning of therapy (the measurement at week 0), and it is clearly impossible to estimate drug effectiveness. The parameter grouping for Model 3 was carefully discussed in [7], using parameter sensitivity analysis and the DAISY tool [12] for checking identifiability of the system after a number of parameters were assumed known. Hence, for Model 3 we choose the following partition of the overall parameters vector:

$$\boldsymbol{\theta}_0 = [\eta_P \ \eta_T \ a \ p \ q \ h \ a_r \ b_r]', \quad \boldsymbol{\theta}_g = [k \ b \ c]', \quad \boldsymbol{\theta}_i = [\lambda_i \ d_i \ u_i]'. \quad (11)$$

It can be noticed that the number of parameters that actually are subject to identification is six, among which three parameters are considered identical for all patients in the same group. For Model 1, given its complete identifiability it is not necessary to set some parameters to values taken from the literature, but it is still useful to distinguish between group dependent and patient dependent parameters. Specifically, we choose for Model 1:

$$\boldsymbol{\theta}_0 = [\eta], \quad \boldsymbol{\theta}_g = [a \ \beta \ k]', \quad \boldsymbol{\theta}_i = [\lambda_i \ d_i \ u_i]'. \quad (12)$$

For Model 2, instead, we choose:

$$\boldsymbol{\theta}_0 = [\eta \quad a \quad p \quad q \quad h],$$

$$\boldsymbol{\theta}_g = [c \quad b \quad \beta]', \quad \boldsymbol{\theta}_i = [\lambda_i \quad d_i \quad \bar{k}_i]'. \quad (13)$$

The identification problem is formulated as the following nonlinear optimization program:

$$\min_{\boldsymbol{\theta}_g, \{T_{0,i}\}_{i=1}^{N_p}} \Phi = \frac{1}{N_p} \sum_{i=1}^{N_p} \sum_{j=1}^{N_m} e'_{i,j} W e_{i,j} \quad \text{s.t.} \quad (14a)$$

$$\boldsymbol{\theta}_g^{\min} \leq \boldsymbol{\theta}_g \leq \boldsymbol{\theta}_g^{\max} \quad (14b)$$

$$\boldsymbol{\theta}_p^{\min} \leq \boldsymbol{\theta}_i \leq \boldsymbol{\theta}_p^{\max} \quad i = 1, \dots, N_p \quad (14c)$$

$$T_0^{\min} \leq T_{0,i} \leq T_0^{\max}, \quad (14d)$$

in which N_p is the number of patients in the group, N_m is the number of available measurement instants, $T_{0,i}$ is time elapsed from infection to beginning of therapy for i -th patient, $W = \begin{bmatrix} 10^{-4} & 0 \\ 0 & 1 \end{bmatrix}$ is the weight matrix that is defined to make numerically comparable the measurements, $\boldsymbol{\theta}_g^{\min}$, $\boldsymbol{\theta}_p^{\min}$, T_0^{\min} ($\boldsymbol{\theta}_g^{\max}$, $\boldsymbol{\theta}_p^{\max}$, T_0^{\max}) specify the lower (upper) bounds (see Tables II, III and IV) for group parameters vector, patient parameters vector, and time elapsed from infection to beginning of therapy, respectively, and:

$$e_{i,j} = \begin{bmatrix} x_i^m(t_j) - x_i(t_j; \boldsymbol{\theta}_0, \boldsymbol{\theta}_g, \boldsymbol{\theta}_i, T_{0,i}) \\ \log_{10} v_i^m(t_j) - \log_{10} v_i(t_j; \boldsymbol{\theta}_0, \boldsymbol{\theta}_g, \boldsymbol{\theta}_i, T_{0,i}) \end{bmatrix}, \quad (15)$$

where $x_i^m(t_j)$ is the measured CD4+ T cell concentration for the i -th patient at time t_j and $x_i(t_j; \boldsymbol{\theta}_0, \boldsymbol{\theta}_g, \boldsymbol{\theta}_i, T_{0,i})$ is the corresponding prediction made with either Model 1, Model 2 or Model 3 using parameters $\boldsymbol{\theta}_0$, $\boldsymbol{\theta}_g$, $\boldsymbol{\theta}_i$ and assuming that:

$$f = \begin{cases} 0 & \text{for } t < T_{0,i} \\ 1 & \text{for } t \geq T_{0,i} \end{cases}. \quad (16)$$

A similar definition applies to the measured viral load $v_i^m(t_j)$ and the corresponding prediction $v_i^m(t_j; \boldsymbol{\theta}_0, \boldsymbol{\theta}_g, \boldsymbol{\theta}_i, T_{0,i})$. If for any i, j both $v_i^m(t_j)$ and $v_i(t_j; \boldsymbol{\theta}_0, \boldsymbol{\theta}_g, \boldsymbol{\theta}_i, T_{0,i})$ are below the detection limit, $e_{i,j}$ is replaced by:

$$e_{i,j} = \begin{bmatrix} x_i^m(t_j) - x_i(t_j; \boldsymbol{\theta}_0, \boldsymbol{\theta}_g, \boldsymbol{\theta}_i, T_{0,i}) \\ 0 \end{bmatrix}. \quad (17)$$

C. Identification problem implementation based on sequential quadratic programming

The range of variability of each parameter is not known precisely, and especially for patient dependent parameter it is expected to be quite large due to a significant inter-patient variability. Therefore, a preliminary identification phase is done by grid search testing each (group and patient) parameter at M points within its range. To ease the search and cope with the large variability, each (group or patient) parameter $\theta \in [\theta^{\min}, \theta^{\max}]$ is expressed in log scale as:

$$\theta(\pi) = \theta^{\min} \left(\frac{\theta^{\max}}{\theta^{\min}} \right)^\pi, \quad \pi \in [0, 1]. \quad (18)$$

It is clear that $\theta(0) = \theta^{\min}$ and $\theta(1) = \theta^{\max}$. Hence, the grid for each parameter is generated by a linear discretization of the corresponding normalized parameter range $[0, 1]$.

TABLE I
VALUES OF COST FUNCTION ACHIEVED BY PRE-IDENTIFICATION PHASE (Φ_0) AND IDENTIFICATION PHASE (Φ^*) FOR MODEL 1 (M1), MODEL 2 (M2) AND MODEL 3 (M3)

	TRU set			MVC set		
	M1	M2	M3	M1	M2	M3
Φ_0	4.04	8.15	3.57	5.97	12.01	7.43
Φ^*	2.52	5.67	3.40	4.91	7.37	5.78

After testing all combinations a parameter values, we obtain a preliminary objective function value Φ_0 . Then, starting from this initial guess we solve problem (14) using a SQP algorithm [13] implemented in GNU Octave. Such an algorithm is guaranteed to generate a sequence of non-increasing function values, and to converge to a (local) minimum of (14). We denote the (locally) optimal function value with Φ^* . It is clear that $\Phi^* \leq \Phi_0$. Moreover, we remark that the pre-identification phase is particularly important (and indeed time consuming) in order to reach a good minimum.

IV. RESULTS AND DISCUSSION

A. Results

The preliminary identification phase and identification phase are applied to the three models, using both TRU and MVC datasets. A tailored code was written for the solution of the preliminary identification phase, while the solution of the identification phase is obtained using the GNU Octave (version 3.6.4) nonlinear optimization routine *sqp*, modified to compute numerical gradients with a step of 10^{-4} instead of the default value about 10^{-8} . For each model and dataset, the solution time of the preliminary identification phase using $M = 4$ grid points for each parameter is in the order of about 60-70 minutes (on an Intel Xeon X5650 2.66 GHz machine running Linux 2.6.37). Then, to complete identification phase less than 5 minutes are necessary.

The preliminary identification phase gives us good sub-optimal initial conditions and allows us to restrict bounds for each parameter in the subsequent identification phase, which is dedicated to refine the search of the optimal values of parameters. As expected, the values of objective function for all the models and datasets are lower after the identification stage with respect to the preliminary phase objective function (see Table I). Model 1 achieves the lowest values of preliminary and optimal cost functions, for both TRU and MVC set; on the contrary, the worst performance, in terms of minimization of the preliminary and optimal cost functions, is obtained by Model 2.

Not all the parameters of each models are found by using the identification phase, mainly because Model 2 and Model 3 are not completely identifiable. The values of these fixed parameters (see Tables II, III and IV) are obtained by the reference papers of each models, and they are invariant with respect to the TRU and MVC set. The effectiveness of therapy is set at the same value (85%) for all models and

TABLE II

MODEL 1: GROUP PARAMETERS, PATIENT PARAMETERS (AVERAGE VALUES), FIXED PARAMETERS AND SEARCHING BOUNDS.

Group parameters	TRU	MVC	bounds
a (1/day)	0.917	0.895	$10^{-3} - 1$
β (1/(day copies μL))	$8.83 \cdot 10^{-7}$	$2.52 \cdot 10^{-7}$	$10^{-7} - 10^{-5}$
k ((copies μL)/(cells mL day))	200	671.01	$2 \cdot 10^2 - 10^3$
Patient parameters	TRU	MVC	bounds
λ (cells/(μL day))	6.77	5.17	$2 - 20$
d (1/day)	0.0132	0.0089	$10^{-3} - 5 \cdot 10^{-2}$
u (1/day)	0.093	0.092	$2 \cdot 10^{-2} - 10$
T_0 (day)	1084	916.4	$56 - 56 \cdot 10^3$
Fixed parameters	TRU	MVC	
η (normalized)	0.85	0.85	

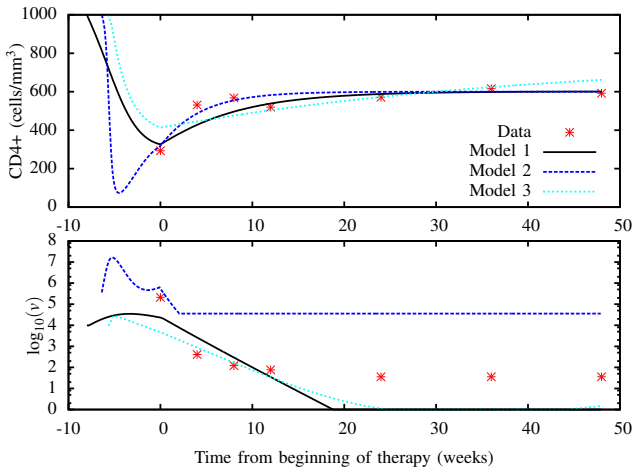


Fig. 1. Example of the identification results obtained for one patient (V001-005) of TRU set, using each of the three models.

datasets. For all considered models, our identification procedure is able to distinguish and characterize the dynamical evolution related to both datasets by means of the differentiation of group dependent parameters. Likewise, the dynamics of each subject are well-followed by the differentiation of patient dependent parameters. Notice that Model 2 shows the lowest differentiation for the group dependent parameters, with respect to the other models. The numerical estimates of both group and patient dependent parameters (see Tables II, III and IV), obtained with our procedure, are significantly different from the ranges reported in literature, [14]–[16]. In Figure 1 we show the outcome of the identification procedure for an illustrative patient (V001-005) from the TRU set, considering all three models. We report in Figure 2 the exemplifying results of the identification phase for one patient of the MVC set (V002-010). For both TRU and MVC sets and for all the models, the CD4+ concentration is well-fitted using the obtained patient dependent parameters. Conversely, the data of viremia are well-fitted only for Model 1 and Model 3, but Model 2 is not able to fit the low values of viremia data.

TABLE III

MODEL 2: GROUP PARAMETERS, PATIENT PARAMETERS (AVERAGE VALUES), FIXED PARAMETERS AND SEARCHING BOUNDS.

Group parameters	TRU	MVC	bounds
c (($\mu\text{L}/\text{cells}$) ² 1/day)	10^{-5}	10^{-5}	$10^{-8} - 1$
b (1/day)	0.0047	0.0060	$10^{-5} - 1$
β (1/(day copies μL))	0.0010	0.0011	$10^{-7} - 10$
Patient parameters	TRU	MVC	bounds
λ (cells/(μL day))	14.80	19.69	$0.5 - 10^2$
d (1/day)	0.03	0.036	$10^{-2} - 0.5$
\bar{k} ((copies mL)/(cells μL))	$9.6 \cdot 10^4$	$1.9 \cdot 10^5$	$10^2 - 10^6$
T_0 (day)	605.3	366.1	$40 - 2 \cdot 10^3$
Fixed parameters	TRU	MVC	
η (normalized)	0.85	0.85	
a (1/day)	0.2	0.2	
p ($\mu\text{L}/(\text{cells day})$)	1	1	
q (cells/ μL)	0.5	0.5	
h (1/day)	0.1	0.1	

TABLE IV

MODEL 3: GROUP PARAMETERS, PATIENT PARAMETERS (AVERAGE VALUES), FIXED PARAMETERS AND SEARCHING BOUNDS.

Group parameters	TRU	MVC	bounds
c (($\mu\text{L}/\text{cells}$) ² 1/day)	$9.8 \cdot 10^{-5}$	$8.8 \cdot 10^{-5}$	$10^{-5} - 10^{-4}$
b (1/day)	0.049	0.0042	$10^{-4} - 5 \cdot 10^{-3}$
k ((copies μL)/(cells mL day))	182.8	109.4	$10^2 - 6 \cdot 10^2$
Patient parameters	TRU	MVC	bounds
λ (cells/(μL day))	7.40	7.54	$1 - 20$
d (1/day)	0.016	0.015	$10^{-3} - 5 \cdot 10^{-2}$
u (1/day)	0.068	0.047	$2 \cdot 10^{-2} - 0.5$
T_0 (day)	283.3	421.2	$40 - 2 \cdot 10^3$
Fixed parameters	TRU	MVC	
η_T (normalized)	0.85	0.85	
η_P (normalized)	0.85	0.85	
a (1/day)	0.1	0.1	
p ($\mu\text{L}/(\text{cells day})$)	2	2	
q (cells/ μL)	100	100	
h (1/day)	0.06	0.06	
b_r (copies/day)	$1.2 \cdot 10^{-8}$	$1.2 \cdot 10^{-8}$	
a_r (1/day)	$1.6484 \cdot 10^{-4}$	$1.6484 \cdot 10^{-4}$	

B. Discussion

It is worth noticing that, for all models, the achieved cost function over the MVC set is higher than that achieved over the TRU set (e.g. for Model 1, Φ^* is equal to 2.52 for TRU set and 4.91 for MVC set). This worse fitting could be associated with a slightly more oscillatory behavior of the measured CD4+ T cells experienced in patients treated with Maraviroc with respect to patients of TRU set, as shown in Figure 2. According to the cost function values, the most effective model appears to be Model 1, followed by Model 3 and then Model 2. These results for Model 1 could be largely expected because such a model is completely identifiable using the available dataset, except for the effectiveness, and indeed we estimated all model parameters.

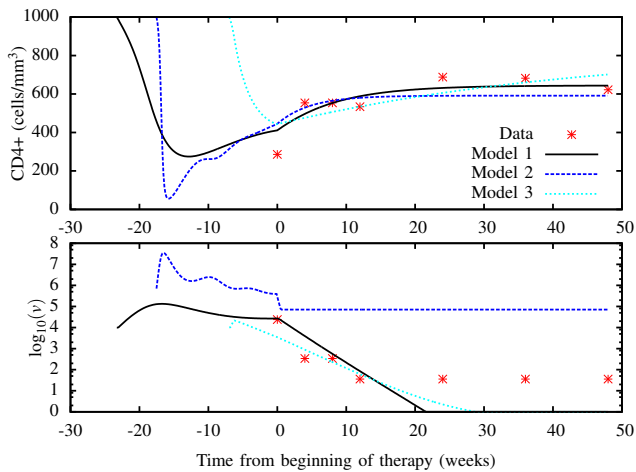


Fig. 2. Example of the identification results obtained for one patient (V002-010) of MVC set, using each of the three models.

For the other models instead, complete identifiability using the same dataset does not hold, and we tried to overcome this limitation by fixing a number of parameters, indicated by sensitivity analysis [7], and estimating the remaining ones. Regarding the worse behavior of Model 2, especially in fitting the viral load, one possible motivation is that it assumes a static relationship between the infected CD4+ T cells and the virus concentration [see Eq. (6)]. As possible remedy, one could use a variant of Model 2 which includes the dynamic evolution of viral load described as in Model 1 and Model 3. In this way, however, such a variant would be very similar to Model 3 (except for the virulence state), and hence the comparison of these three models could be less interesting. Finally, in the comparison between Model 1 and Model 3, it should be highlighted that the slightly higher cost function of Model 3 is mainly due to a worse fitting of the first viral load measurement. In particular, if we excluded the error of the first viral load measurement (or give it a lower weight) the cost function values of Model 1 and Model 3 would be almost equal.

V. CONCLUSIONS AND OUTLOOK

Our work represents only a first step towards a deeper knowledge of different models with respect to practical identification of their parameters. A traditional rule of modeling is that if two models lead to the same error you should prefer the simplest one; this rule represents the guideline also in the case of HIV models, where the compromise between limited data and practicability of the identification procedure should be taken into account. Our study follows the criterion to compare different models in terms of the minimization of the weighted sum of square fitting errors for CD4+ and viral load for the same dataset of patients. We would like to point out that, at the best of our knowledge, in previous studies for homogeneous dataset a comparison between mathematical models to identify and validate HIV evolution models has not been performed. The conclusions of this paper cannot lead to an ultimate decision on the best choice among HIV models: more research activity needs to

be carried out, e.g. using a higher number of models and a larger dataset. Nevertheless it is interesting to note that both the earlier three state model and the more complex virulence-based model fit satisfactorily the two datasets. On the other hand the virulence model has a more complete and flexible structure and it could be used for different HIV species and for studying the immune system and possible viral mutations, also in cases of different therapeutic actions. We expect that this work stimulates more researches in this comparative direction.

VI. ACKNOWLEDGEMENTS

We gratefully acknowledge Dr. G. Tambussi and Dr. S. Nozza from San Raffaele Research Institute (Milan, Italy) who provided the clinical data for this study.

REFERENCES

- [1] A. S. Perelson and P. W. Nelson, "Mathematical analysis of HIV-I: Dynamics in vivo," *SIAM Review*, vol. 41, no. 1, pp. 3–44, 1999.
- [2] J. W. Eaton, L. F. Johnson, J. A. Salomon, and et al., "HIV treatment as prevention: systematic comparison of mathematical models of the potential impact of antiretroviral therapy on HIV incidence in south africa." *PLoS Medicine*, vol. 9, no. e1001245, 2012.
- [3] X. Xia and C. H. Moog, "Identifiability of nonlinear systems with application to HIV/AIDS models," *IEEE Trans. Auto. Contr.*, vol. 48, no. 2, pp. 330–336, 2003.
- [4] M. A. Nowak and C. R. Bangham, "Population dynamics of immune responses to persistent viruses." *Science*, vol. 272, no. 74–79, 1996.
- [5] D. Wodarz and M. A. Nowak, "Mathematical models of HIV pathogenesis and treatment," *BioEssays*, vol. 24, pp. 1178–1187, 2002.
- [6] —, "Specific therapy regimes could lead to long-term immunological control of HIV," *Proc. Natl. Acad. Sci. USA*, vol. 96, pp. 14464–14469, 1999.
- [7] G. Pannocchia, E. Morano, M. Laurino, S. Nozza, G. Tambussi, and A. Landi, "Identification and experimental validation of an HIV model for HAART treated patients," *Comput. Methods and Programs Biomed.*, vol. 112, no. 3, pp. 432–440, 2013.
- [8] G. Pannocchia, M. Laurino, and A. Landi, "A model predictive control strategy towards optimal structured treatment interruptions in anti-HIV therapy," *IEEE Trans. Biom. Eng.*, vol. 57, no. 5, pp. 1040–1050, 2010.
- [9] A. Landi, A. Mazzoldi, A. Chiara, M. Bianchi, A. Cavallini, M. Laurino, L. Ricotti, R. Iuliano, B. Matteoli, and L. Ceccherini-Nelli, "Modelling and control of HIV dynamics," *Comput. Methods Programs Biomed.*, vol. 89, no. 2, pp. 162–168, 2008.
- [10] X. Xia, "Estimation of HIV/AIDS parameters," *Automatica*, vol. 39, pp. 1983–1988, 2003.
- [11] S. Nozza, L. Galli, A. Antinori, M. Di Pietro, C. Tommasi, M. Zaccarelli, R. Fezza, S. Bonora, G. Tambussi, and A. Lazzarin (VEMAN Study Group), "Maraviroc 150 mg QD plus lopinavir/ritonavir, a NRTIs-sparing regimen for naïve patients: preliminary 48-weeks results," in *6th International AIDS Conference on HIV Pathogenesis, Treatment and Prevention*, Rome (Italy), 2011, p. no. CDB325.
- [12] G. Bellu, M. P. Saccomani, S. Audoly, and L. D'Angiò, "DAISY: a new software tool to test global identifiability of biological and physiological system," *Comput. Methods Programs Biomed.*, vol. 88, pp. 52–61, 2007.
- [13] J. Nocedal and S. J. Wright, *Numerical Optimization*, 2nd ed. Springer, 2006.
- [14] H. Putter, S. Heisterkamp, J. Lange, and F. De Wolf, "A bayesian approach to parameter estimation in HIV dynamical models," *Statistics in medicine*, vol. 21, no. 15, pp. 2199–2214, 2002.
- [15] H. Huang, C.-C. Liu, and X. J. Zhou, "Bayesian approach to transforming public gene expression repositories into disease diagnosis databases," *Proceedings of the National Academy of Sciences*, vol. 107, no. 15, pp. 6823–6828, 2010.
- [16] R. Luo, M. J. Piovoso, J. Martinez-Picado, and R. Zurakowski, "HIV model parameter estimates from interruption trial data including drug efficacy and reservoir dynamics," *PLoS one*, vol. 7, no. 7, p. e40198, 2012.